Supplementary materials

Sparse Odor Representation and Olfactory Learning

Iori Ito, Rose Chik-ying Ong, Baranidharan Raman, and Mark Stopfer

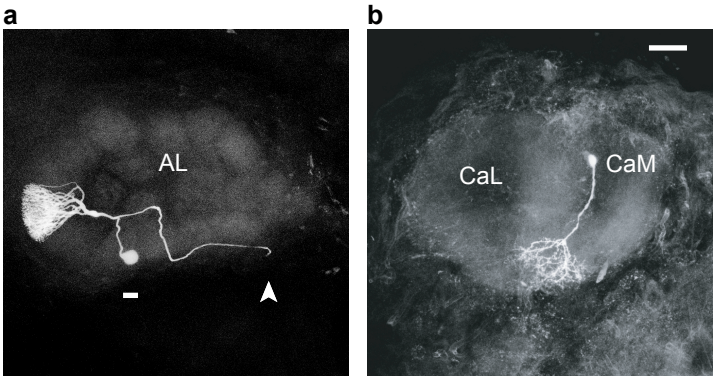

Supplementary Fig. 1 Morphological identification of cell type.
After physiological characterization, we injected fluorescent dye for morphological analysis of the recorded cell. Projection images of confocal stacks are shown. (**a**) Example of projection neuron morphology; anterior view of antennal lobe; projection neuron filled with Lucifer-yellow. The neuron's shape and the process exiting the antennal lobe (arrowhead) are characteristics of projection neurons. AL: antennal lobe. Scale bar: 20 μm. (**b**) Example of Kenyon cell morphology, posterior view of mushroom body; Kenyon cell filled with Lucifer-yellow. Scale bar: 50 μm. CaM: medial calyx; CaL: lateral calyx.

For intracellular recordings, the tip of the micropipette was filled with a 5% solution of Lucifer yellow CH in 0.2 M LiCl, or with a 10 mM solution of one of the Alexa Fluor hydrazides (Alexa Flour 488, Alexa Flour 568, Alexa Flour 633, Invitrogen, Carlsbad, CA) in 0.2M KCl. The electrode shaft was filled with 0.2 or 0.5 M LiCl. In some experiments, a 5% solution of neurobiotin (Vector Labs; Burlingame, CA) in 0.5 M potassium acetate was used to fill the tip and shaft of the microelectrode. Intracellular recordings were amplified in bridge mode (Axoclamp-2B, Axon Instruments, Foster City, CA). Intracellular signals were acquired at 5 kHz using PCI-MIO-16E-4 DAQ cards (National Instruments, Austin, TX) and custom LabVIEW software (National Instruments).

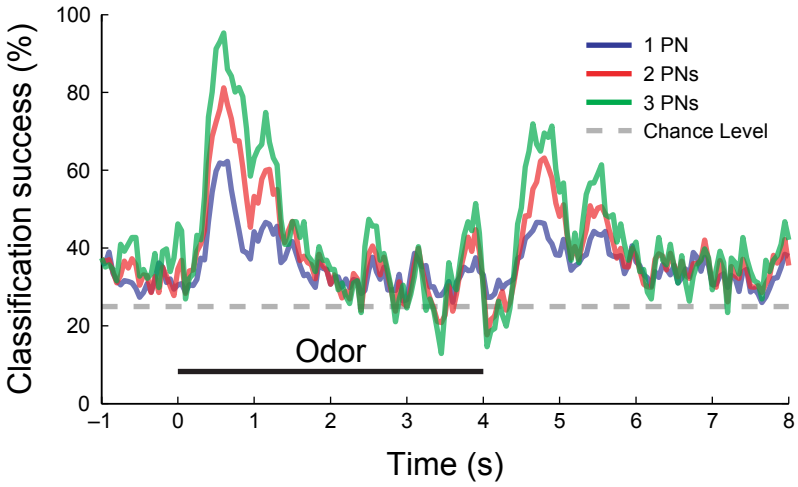

Supplementary Fig. 2 Projection neuron firing patterns reliably contain information about odors.
Classification success rates averaged over projection neuron-odor combinations (see **Supplementary Methods**) plotted over time. Classification success was greatest at odor onset and offset. Classification success based upon the activity of a single projection neuron greatly exceeded chance level (25%), indicating that odors induced reliable and odor-specific firing activity. The classification success rate increased with the number of projection neurons, indicating that ensembles of projection neurons can encode the stimulus more reliably. Black horizontal bar: odor presentation.

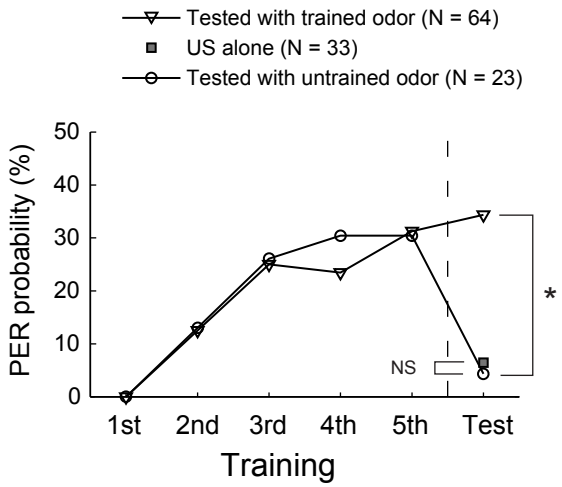

Supplementary Fig. 3 Trained moths learned about odors, not other non-specific cues. We trained two groups of moths with benzylaldehyde or cyclohexanone in the On/Off response procedure with 2 s ISI. In each group, half the animals were trained with each odor. After the training, we tested one group with the trained odor and the other group with the untrained odor. Moths responded only to the trained odor, not to the untrained odor. We determined statistical significance by Fisher's exact test with Bonferroni-corrected *P* values.

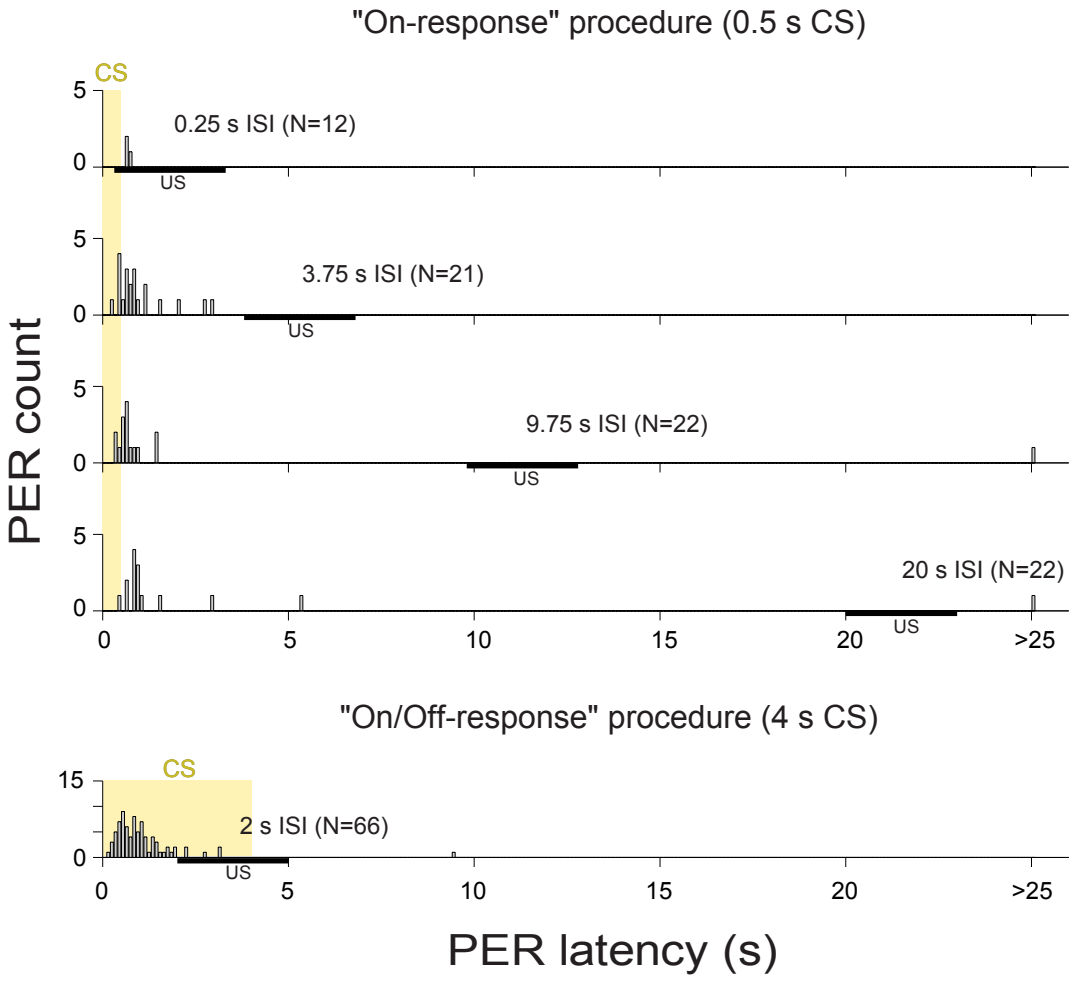

Supplementary Fig. 4 Moths responded to odor onset regardless of reward timing. In these experiments, we measured the latencies of all PER responses during training and testing from video recordings. We trained different groups of moths with different CS-US intervals. Most moths quickly responded to the odor pulse (the CS) within 1 s regardless of the training interval. Frequency histograms show time after odor onset when the start of proboscis extension was noted. The bins labeled > 25 s include responses occurring between 25 s and 60 s after CS onset. N: number of moths in the group. Yellow boxes: the CS presentation time. Black horizontal bars under histograms: the US (sucrose) presentation time.

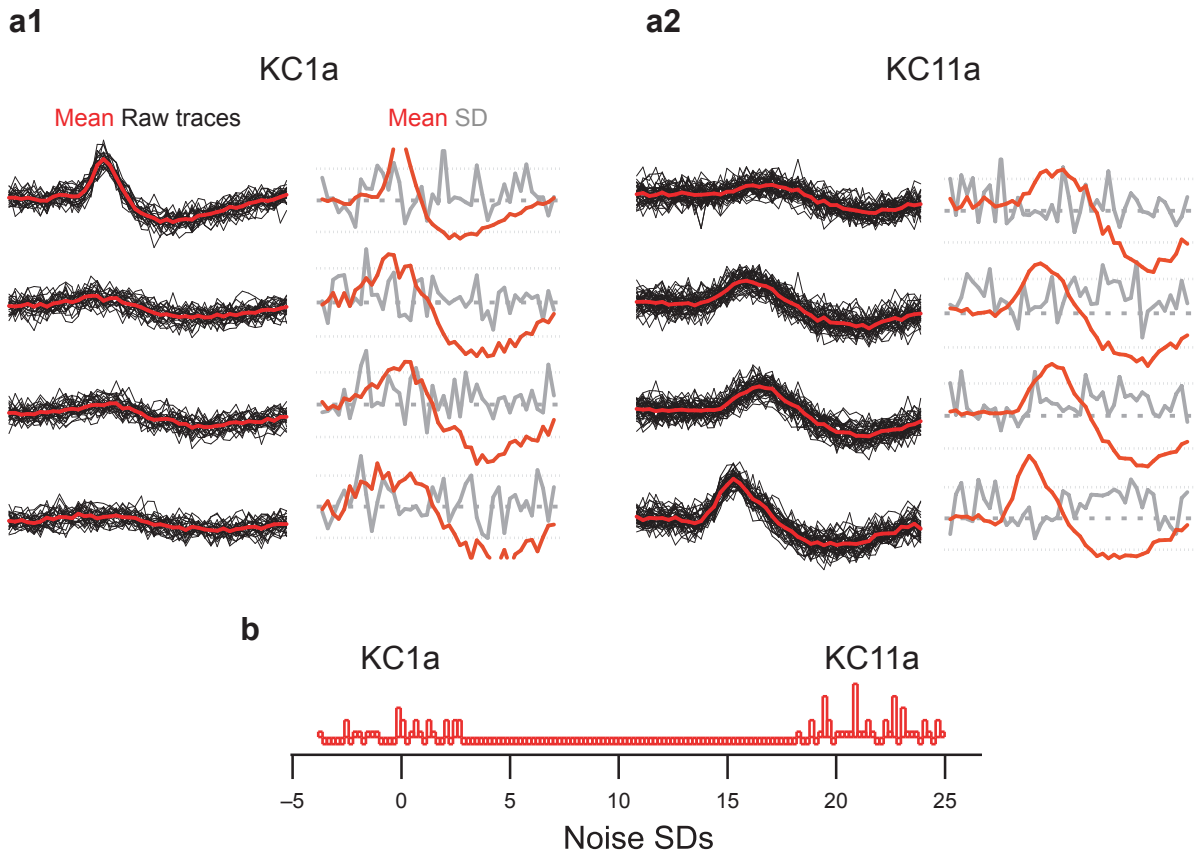

Supplementary Fig. 5 Examples of spike sorting.
We performed spike sorting conservatively, taking into account the full waveform of each spike event from four channels[43]. We made extracellular recordings of Kenyon cell activity using custom-made twisted wire tetrodes. To collect a representative sample of Kenyon cells, electrodes were placed at random locations within the mushroom body. Spike sorting was achieved offline, using the best 4 of the 8 channels recorded, and consistent with conservative statistical principles[43] (Spike-o-Matic) implemented in IGOR Pro (Wavemetrics, Lake Oswego, OR). A total of 266 Kenyon cells (117 for **Fig. 2f**, another 117 for **Fig. 3a**,**b** and 32 more for **Fig. 3c**,**d**) were recorded from 36 moths of either sex. In most cases, both right and left sides of the mushroom bodies were tested in each animal.

(**a**) Example of individual events (black), their mean (red), and the SD (gray) in each of the four channels for all events classified as KC1a (**a1**) and KC11a (**a2**), respectively. (**b**) Histogram obtained by projecting KC1a and KC11a events onto the line connecting their means. We considered only well separated clusters, with centers separated by at least five times the noise SD.

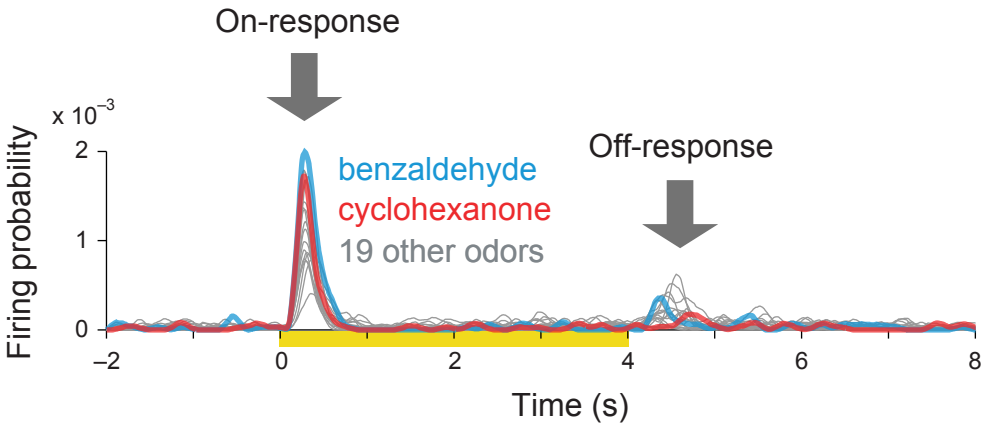

Supplementary Fig. 6 All odors, including those used to test behavior, evoked similar temporal spiking characteristics in Kenyon cells.
Each line represents a histogram (bin size: 1 ms) that combines 1,170 trials from 117 cells. Odors used for behavioral training (benzaldehyde and cyclohexanone) evoked overall temporal activity patterns in Kenyon cells (strong on-responses and much weaker off-responses) similar to those of all other odors tested. Yellow bar: odor presentation.

Supplementary Methods

Histology

After electrophysiological characterization, we stained cells by passing current pulses (for fluorescent dyes – 1 to – 10 nA, 0.5 s duration, 1 Hz; for neurobiotin + 3 nA, 0.5 s duration, 1 Hz) for 5–40 min. We then fixed brains with 4% paraformaldehyde in phosphate buffer (pH 7.4) overnight. We visualized neurobiotin by incubating brains overnight in a 0.1% solution of streptavidin-Alexa conjugate in phosphate buffer containing 1% Triton (Alexa-Fluor-568 or 633 conjugated streptavidin, Invitrogen). We dehydrated fixed brains through a graded ethanol series and cleared with methyl salicylate. We imaged the brains with a laser-scanning confocal microscope (LSM 510 Upright 2-Photon Meta, Carl Zeiss Inc., Thornwood, NY) equipped with a 458 Argon ion laser, a 543 nm Helium-Neon laser, and a 633 nm Helium-Neon laser. We obtained projection images of confocal stacks using the projection function of Zeiss LSM Image Browser version 4.2.0.121 (Carl Zeiss Inc) in transparent mode.

Classification analysis

To test the reliability and information content of projection neuron firing patterns, we performed a standard classification analysis[4] using single and multiple projection neuron ensemble responses (up to 3 projection neurons) based upon dataset shown in **Fig. 1**. Among the 62 projection neuron-odor combinations, we included only those projection neuron singlets, pairs, and triplets that were tested for the same three odors at least three trials for each odor for this analysis. This resulted in a total of 227 combinations for classification based on single projection neuron activity, 88 and 19 combinations for projection neuron pair and triplet cases, respectively (each combination represents a separate classification problem).

We constructed a response vector by concatenating projection neuron firing rates in five consecutive 50 ms bins (250 ms activity) from single or multiple projection neurons. To predict the odor label of a response vector in the test trial, we computed the Euclidean distance between the test trial response vectors with each of the remaining trials (corresponding response vectors); we then assigned the test vector the odor label of the closest trial (smallest Euclidean distance). We used the first three trials for each of the three odors (a total of 9 trials), thus each classification task had one test trial and 8 remaining trials. Therefore, the classification success by chance was 25% (2 out of 8). We used a standard leave-one out validation method to ensure every trial served as a test trial in the classification analysis. We averaged the classification rates across different combinations. We repeated this analysis for 50 ms step sliding windows over the course of each trial. We obtained similar results with a range of bin sizes.

Projection neuron activities at odor onset and offset supported successful odor classification that significantly exceeded chance level (25%). We judged statistical significance ($P < 0.05$) by estimating the probability of getting the

observed classification success probability or higher, assuming a random binomial process. We performed the analysis separately for singlet, pair and triplet projection neuron ensembles.

Video analysis

In some experiments, we recorded training and testing with a digital video camcorder (PV-GS400, Panasonic, Japan) at 29 frames/s. Odor onset was indicated by a flashing LED controlled by the odor pulse generator; we defined proboscis extension response (PER) latency as the time difference from the first frame showing the LED illuminated to the first frame showing the beginning of a proboscis extension response. We measured timing with video processing software (VirtualDub 1.6.17, http://www.virtualdub.org). We measured the latencies of all PER responses during training and test phases except for the first training trials to exclude spontaneous PERs.